Local Administration of Porcine Immunomodulatory, Chemotactic and Angiogenic Extracellular Vesicles using Engineered Cardiac Scaffolds for Myocardial Infarction

Marta Monguió-Tortajada†, Cristina Prat-Vidal†, Miriam Moron-Font, Marta Clos-Sansalvador, Alexandra Calle, Paloma Gastelurrutia, Adriana Cserkoova, Anna Morancho, Miguel Ángel Ramírez, Anna Rosell, Antoni Bayes-Genis, Carolina Gálvez-Montón*, Francesc E. Borràs*, Santiago Roura*

Supplementary Figures

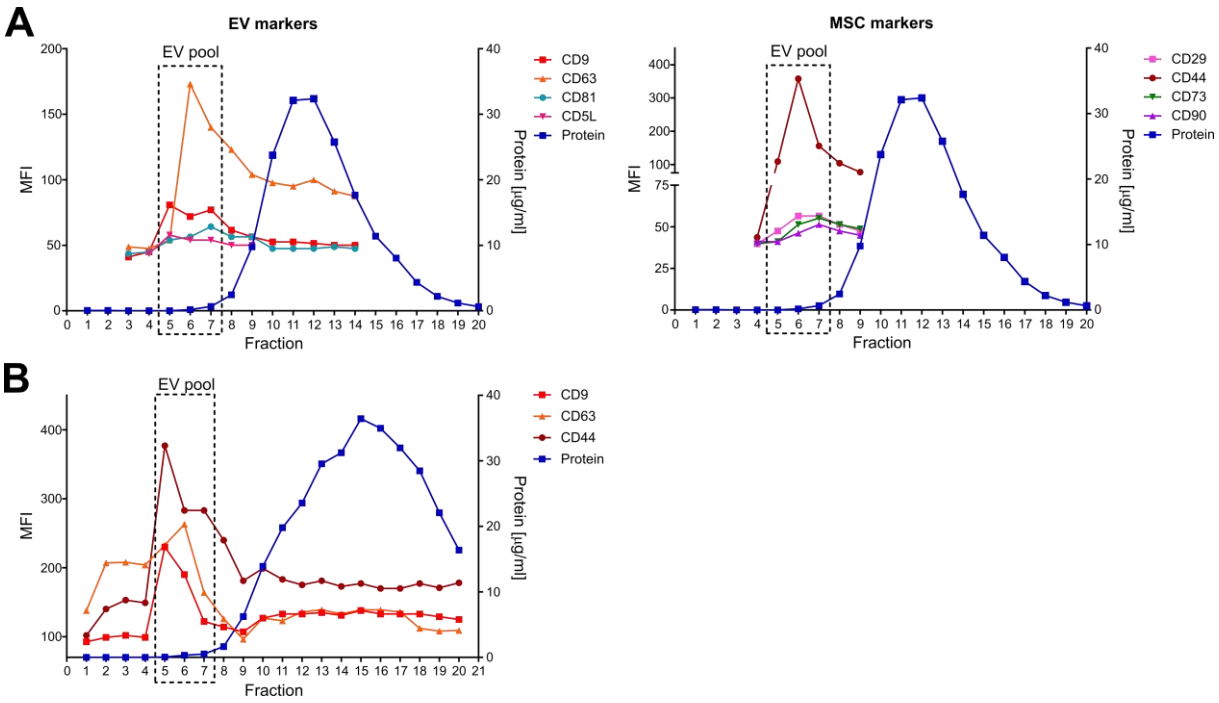

FIGURE S1 | cATMSC-EV were positive for EV markers ($CD9^{+}$ $CD63^{+}$ $CD81^{low}$ $CD5L^{low}$) and MSC markers ($CD44^{+}$ $CD29^{low}$ $CD73^{low}$ $CD90^{low}$). (**A**) The screening for EV (left) and MSC (right) markers on cATMSC-EV eluting in 1ml-SEC columns indicated that anti-CD63 and anti-CD44 were the most suitable antibodies to be used for porcine cATMSC-EV detection. (**B**) The EV marker CD9 was tested again, and indicated that porcine cATMSC-EV could be detected as $CD63^{+}$ $CD9^{+}$ $CD44^{+}$.

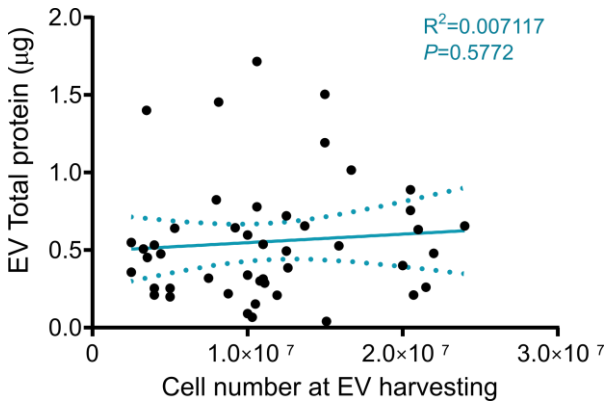

FIGURE S2 | Lack of correlation between the total protein quantified in the EV pool and the EV-producing cell number at harvest.

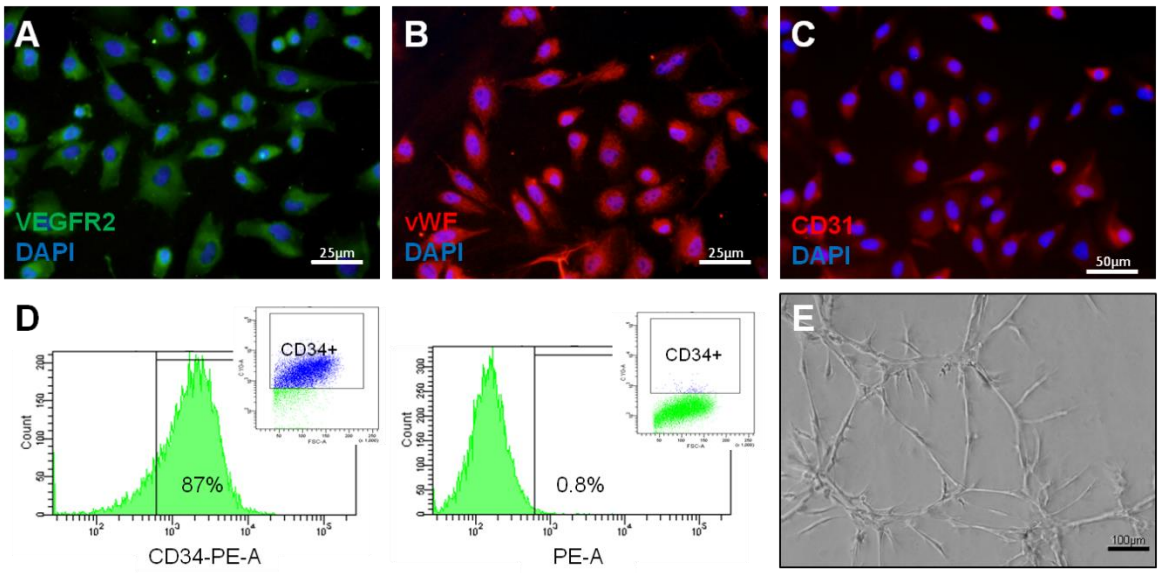

FIGURE S3 | Porcine outgrowth endothelial cell (OEC) characterisation. **(A–D)** Endothelial and hematopoietic lineage cell markers were analysed by immunocytochemistry **(A–C)** and flow cytometry **(D)**, respectively. Representative images of OECs immunostained for **(A)** vascular endothelial growth factor receptor 2 (VEGFR2; green), **(B)** von Willebrand Factor (vWF; red), or **(C)** platelet/endothelial cell adhesion molecule (CD31; red), and nuclei stained with DAPI (blue). **(D)** Representative flow cytometry plots of CD34-labeled OECs or negative control (right panel). Cells were positive for endothelial markers VEGFR2, vWF and CD31, and for the progenitor/hematopoietic marker CD34 (>85%). **(E)** Matrigel assay showing that OECs formed vessel-like structures after 24 h.

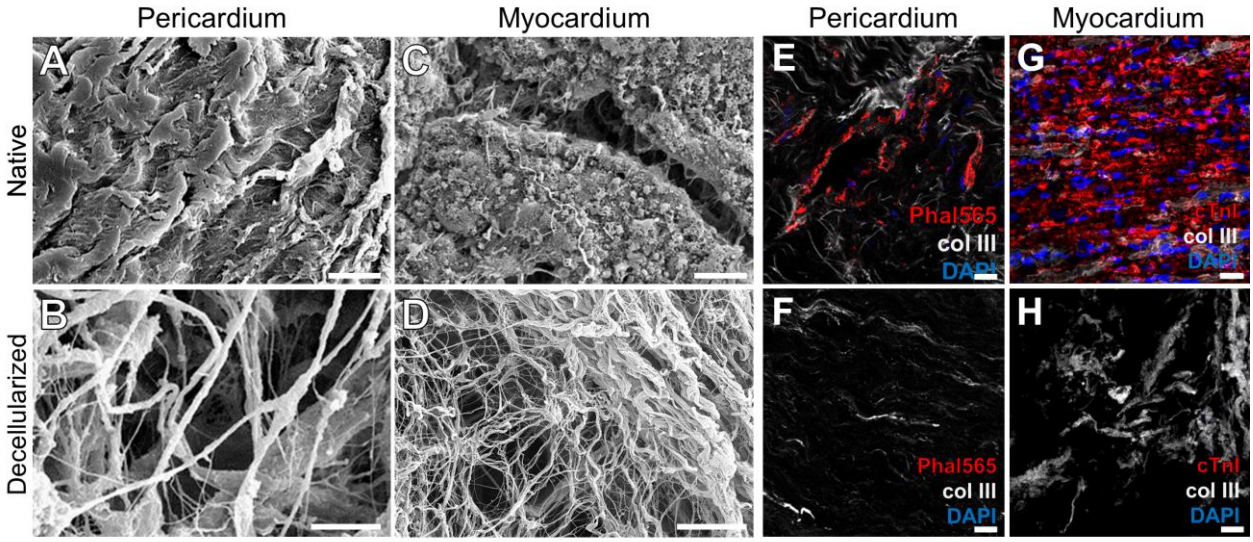

FIGURE S4 | 3D bioengineered scaffolds maintain their internal ultrastructure and are devoid of cells after decellularisation. Ultrastructure determined by scanning electron microscopy (SEM) of the **(A)** native pericardium and **(B)** decellularised pericardial scaffolds; or **(C)** native myocardium and **(D)** decellularized myocardial scaffolds. Scale bars = 10 μm. **(A)** Image of the fibrous side of the parietal pericardium showing mesothelial elongated cells with oblique orientation (upper left) covering part of the fibrosa (lower right). **(C)** Cross section of porcine left ventricle, with visible myofibrils in the cytoplasm of cardiac muscle cells, separated by loose stromal connective tissue. **(E, F)** Representative images of the native pericardium and decellularised pericardial scaffolds, respectively; and **(G, H)** native myocardium and decellularised myocardial scaffolds showing immunostaining for phalloidin (Phal565, red), cardiac troponin I (cTnI, red), and collagen III (col III, grey). Decellularisation is indicated by the absence of actin filaments or cTnI, and cell nuclei (DAPI, blue). Scale bars = 20 μm.

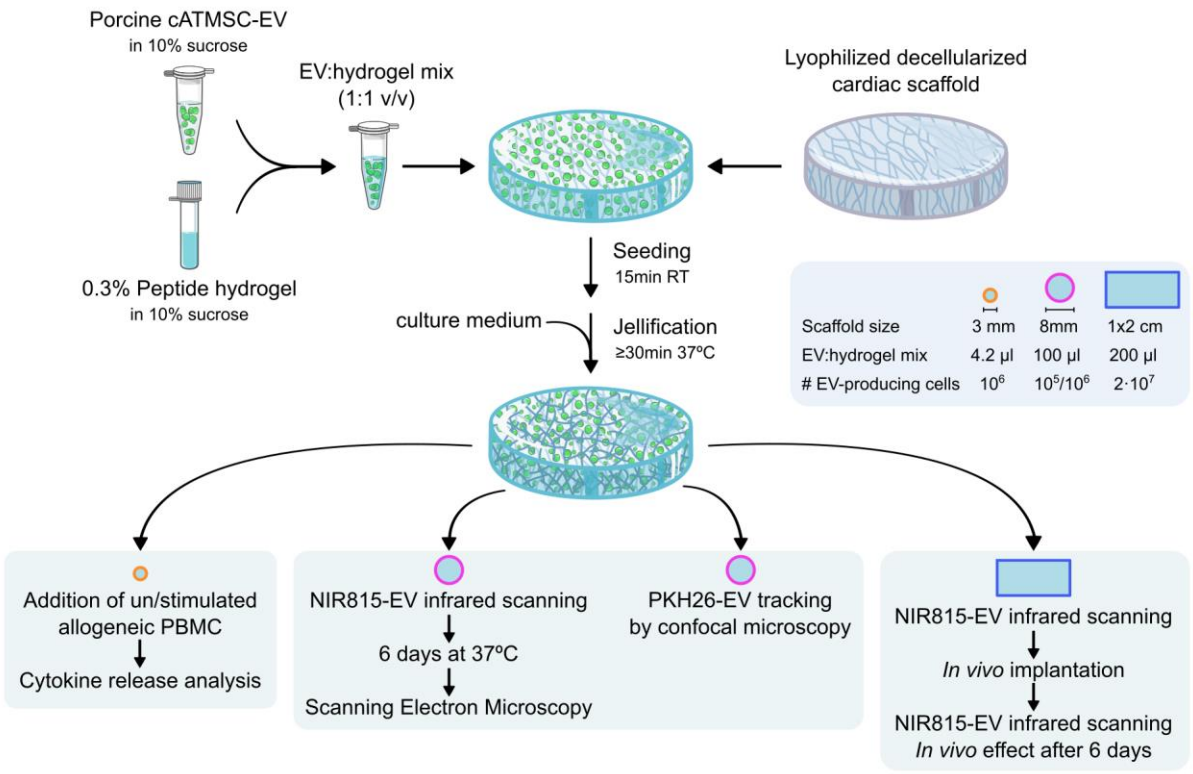

FIGURE S5 | Schematic summary of cATMSC-EV loading in cardiac scaffolds with peptide hydrogel. Porcine cATMSC-EV (green) of a specific number of EV-producing cells were mixed 1:1 (v/v) with 0.3% Puramatrix self-assembling peptide hydrogel (both in 10% sucrose) and loaded into lyophilized, decellularized myocardial or pericardial scaffolds. After 15 min of seeding and scaffold rehydration, the salt-triggered hydrogel jellification was promoted by adding culture medium. Then, cATMSC-EV-loaded scaffolds were used or processed for the outlined experimental purposes. The different scaffold sizes with the respective volumes of cATMSC-EV:hydrogel mix and corresponding EV-producing cell numbers are indicated.

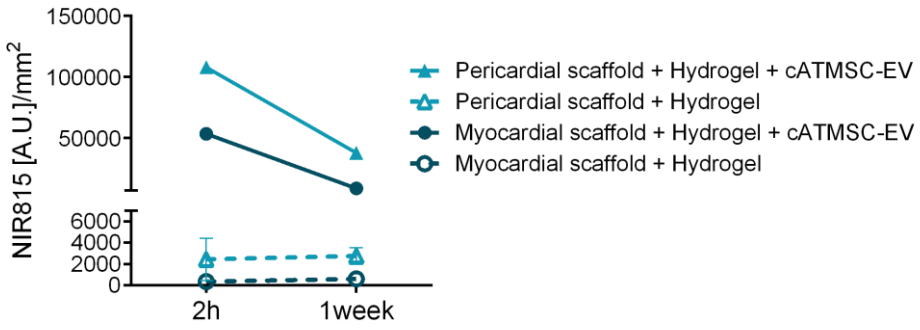

FIGURE S6 | Fluorescent signal within scaffolds filled with cATMSC-EV labelled with NIR815 embedded in peptide hydrogel decreases after a week in culture.

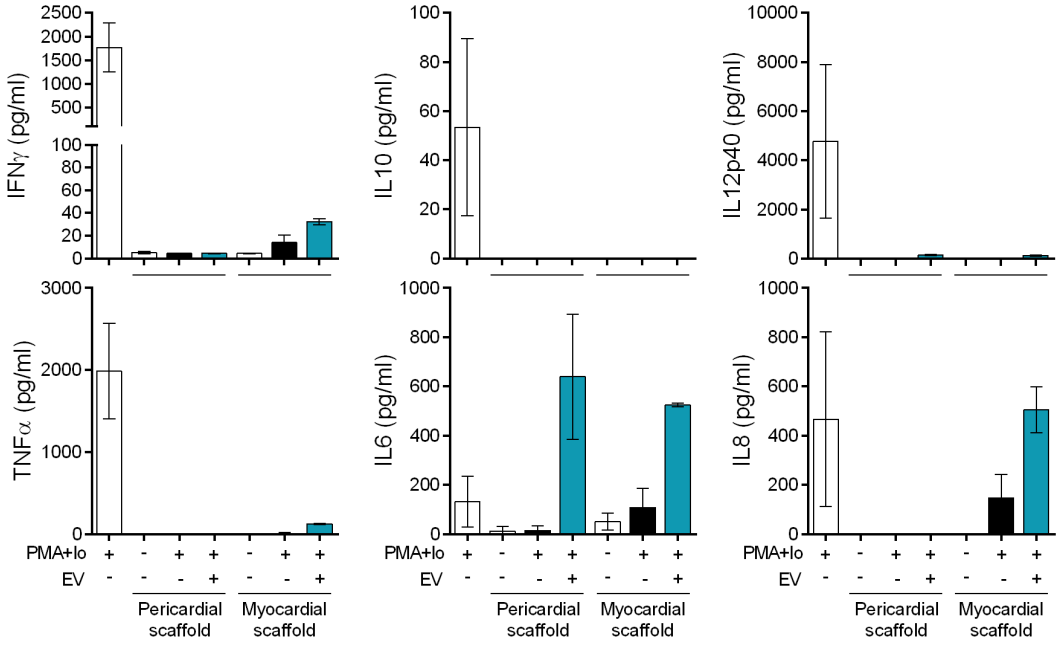

FIGURE S7 | Porcine cATMSC-EV embedded in cardiac scaffolds modulate cytokine responses of third-party PBMC after polyclonal stimulation. Cytokine levels of supernatants of $1x10^5$ PBMC after five days after PMA + Io stimulation in the presence or absence of pericardial or myocardial scaffolds filled with cATMSC-EV (from $1x10^6$ cATMSC) mixed with peptide hydrogel. Data points represent the average of two biological replicates. Horizontal bars indicate the mean ± SD.

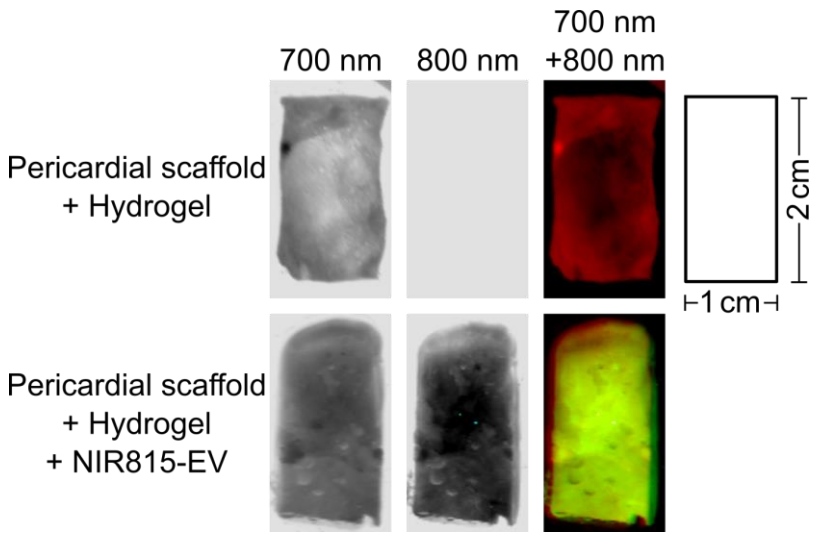

FIGURE S8 | Fluorescence of NIR815-labelled cATMSC-EV was confirmed in loaded pericardial scaffolds before implantation in animals. Pericardial scaffolds of 2 cm^2 were loaded with peptide hydrogel mixed with 10% sucrose buffer (Control animals; top) or NIR815-labelled cATMSC-EV (Treated animals; bottom). Representative scanning images of pericardial scaffolds autofluorescence at 700 nm (left, and red on the right) and NIR815 fluorescence at 800 nm (middle, and green on the right).

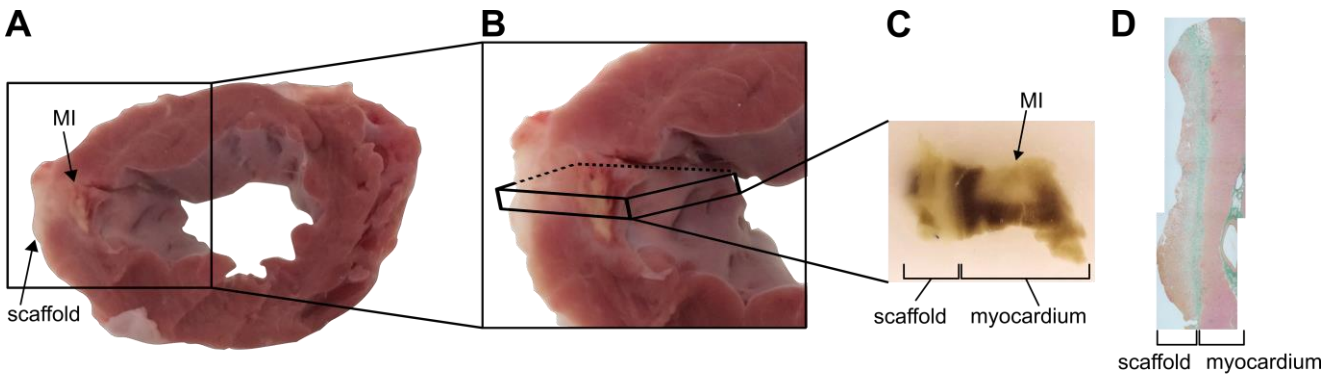

FIGURE S9 | Tissue collection for histological and immunohistofluorescence examination. Excised hearts were washed in saline buffered solution to remove any residual blood, sliced transversely into 1-cm sections **(A)** from artery ligation to the apex, and digitally photographed for morphometric analysis. **(B)** Then, tissue transverse samples (5 mm) from the middle of the scar were cut and selected based on macroscopical examination of each slice, and either fixed in 10% formalin for paraffin inclusion **(C)** or embedded in OCT and snap-frozen in liquid nitrogen-cooled isopentane **(D)**. **(C-D)** The scaffold, although already integrated in the myocardium, was easily distinguishable by gross examination. The myocardial tissue of each slice included infarct core (MI), border zones and healthy non-scarred tissue. **(D)** Representative mosaic image reconstruction of a tissue section after Masson's trichrome staining, showing the scaffold (left) and myocardium (right) junction (epicardium).

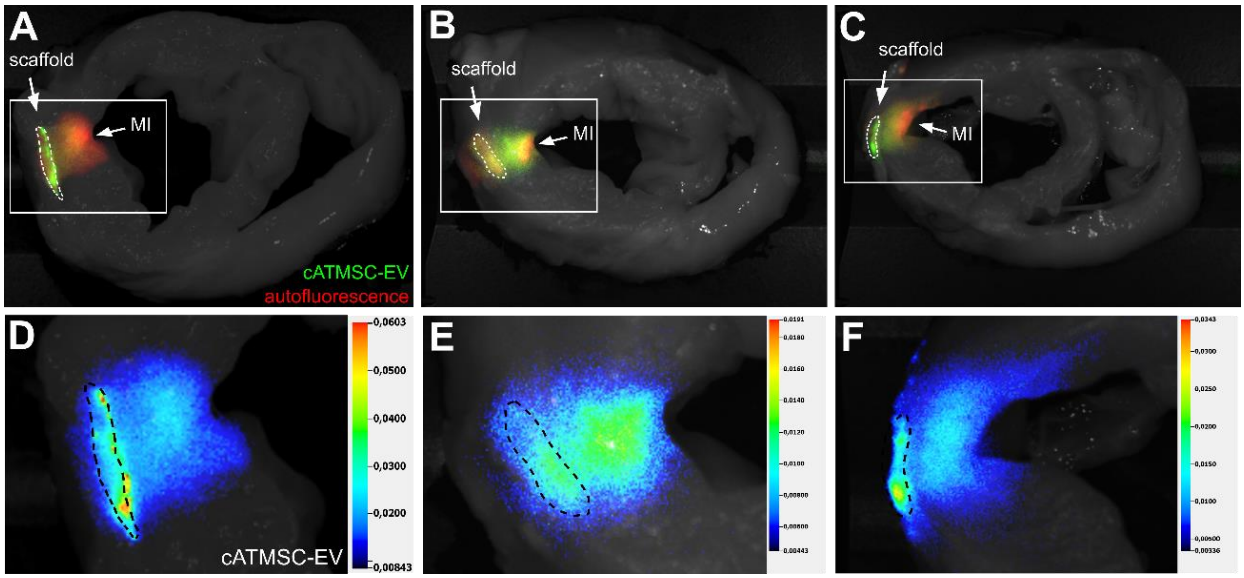

FIGURE S10 | Porcine NIR815-cATMSC-EV detection in the scaffold and infarct area in the three treated animals after six days post-implantation. **(A-C)** Administered NIR815-cATMSC-EV (green; 800 nm) are detected within the scaffold (white dotted line) and MI core (red; autofluorescence; 700 nm) by fluorescent tracking. Both fluorescent signals are overlaid on a white light image of the heart section. **(D-F)** Close-up pseudo-colour intensity images depicting NIR815-EV signal at the 800 nm channel within the scaffold (black dotted line) and MI core. *Related to Figure 6.*

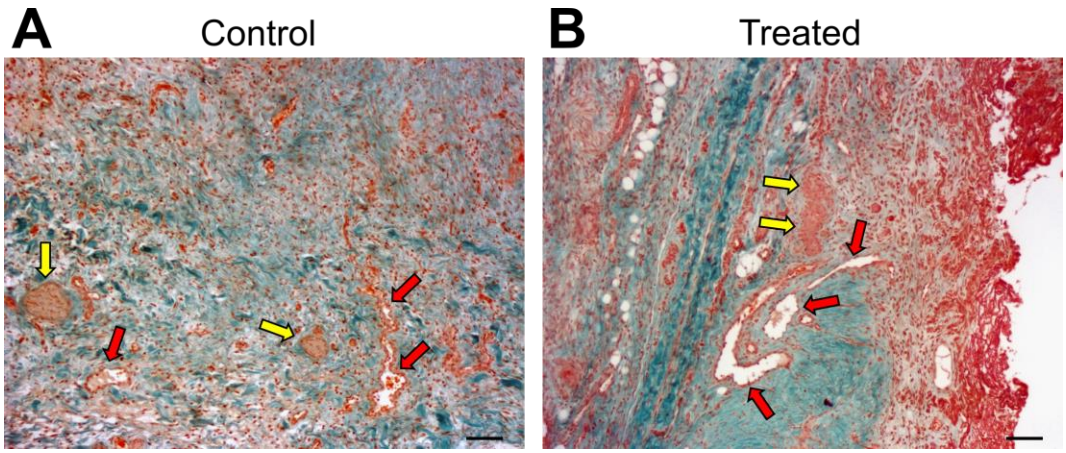

FIGURE S11 | Representative images of light green Masson's trichrome staining of control **(A)** and treated **(B)** animals showing the de novo formation of vessels (red arrows) and nerves (yellow arrows) within the post-implanted scaffolds. Scale bar = 100 µm.

SUPPLEMENTARY VIDEO 1 | 20-h lapse video of swine peripheral blood outgrowth endothelial cells (OEC) in contact with a control (10% sucrose buffer) agarose spot. OEC do not enter the spot, and delocalise away from the spot border to find available surface for attachment.

SUPPLEMENTARY VIDEO 2 | 20-h lapse video of swine peripheral blood outgrowth endothelial cells (OEC) in contact with a VEGF-containing agarose spot. Some OEC can be seen entering the spot and actively migrating towards its centre.

SUPPLEMENTARY VIDEO 3 | 20-h lapse video of swine peripheral blood outgrowth endothelial cells (OEC) in contact with an agarose spot containing porcine cardiac adipose tissue-derived mesenchymal stem cell extracellular vesicles (cATMSC-EV). cATMSC-EV recruit OEC, as they can be seen entering the spot and actively migrating towards its centre.

SUPPLEMENTARY VIDEO 4 | 20-h lapse video of allogeneic swine cATMSC in contact with a control (10% sucrose buffer) agarose spot. cATMSC do not enter the spot, and delocalise away from the spot border to find available surface for attachment.

SUPPLEMENTARY VIDEO 5 | 20-h lapse video of allogeneic swine cATMSC in contact with an agarose spot containing porcine cardiac adipose tissue-derived mesenchymal stem cell extracellular vesicles (cATMSC-EV). cATMSC-EV recruit allogeneic cATMSCs, as they can be seen entering the spot and actively migrating towards its centre.

SUPPLEMENTARY VIDEO 6 | 20-h lapse video of allogeneic swine cATMSC in contact with an agarose spot containing porcine cardiac adipose tissue-derived mesenchymal stem cell extracellular vesicles (cATMSC-EV). A higher cATMSC-EV concentration yields an increased allogeneic cATMSC recruitment towards the center of the EV-containing agarose spot.